# LATEST RESULTS FROM THE CLIC GEODETIC STUDIES

M. Jones, CERN, Geneva, Switzerland
J. Boerez, EOST, Université de Strasbourg, France / CERN, Geneva, Switzerland
S. Guillaume, GGL, ETH Zurich, Switzerland / CERN, Geneva, Switzerland
Dr. J. Hinderer, Dr. L. Rivera, EOST, Université de Strasbourg, France
Dr. B. Bürki, GGL, ETH Zurich, Switzerland

*Abstract*

The alignment challenge presented by the CLIC* project requires us to look closely at the gravity field and our ability to model the geoid and the influence of tidal and other non-periodic effects. This is of particular importance if we wish to use Hydrostatic Levelling Systems (HLS) in the alignment system, and may have a bearing on the use of other instruments too. To examine how the gravity field can directly affect an accelerator's alignment two research projects are currently underway.

The first is a study to determine the geoidal undulations along a straight line as accurately as possible, and to understand if significant local undulations are even possible. The geoid determination is centred on the use of a high precision astro-geodetic camera, coupled with gravimetric measurements at the surface and in a tunnel ~100 m directly below. The first measurement campaign has been completed and the preliminary results will be presented.

The second study looks at the tidal (and other) effects on measurements made with an HLS. Many factors could affect the alignment of an accelerator over a length of several hundred metres, but we are only interested in those which can produce significant local deformations. An analysis of the contributing factors has been made, different approaches have been considered and tried, and the results to date will be presented.

## INTRODUCTION

HLS systems have been used for accelerator alignment for many years now. They have the great advantage of providing a vertical reference surface from which certain sensors can measure their distance with a micrometric accuracy. Obviously, HLS are not referred to a straight line but to the instantaneous shape of the water surface in the pipes, and the difficulty lies is determining the form of that surface to the required level of accuracy. Physically this can be formulated as determining the instantaneous equipotential surface of the Earth's gravity field at the level of the water.

However, that will not be sufficient if we are to use these instruments to maintain the long term alignment of an accelerator. In that case the variations in the equipotential surface as a function of time are also required, a phenomena which is primarily explained by the Earth Tides, but which is also influenced by other effects. In fact these tidal effects can affect the surface on which the accelerator is placed (e.g. tunnel floor) differently to the water surface in the HLS and this must also be taken into account.

For the CLIC alignment, HLS are planned to be used for the main metrological network which should be able to give a reference with respect to a straight line in Euclidean space with a relative precision of 10 microns over 200 meters.

The primary consequence is that it forces us to determine the effect of the Earth's mass distribution and it's motion within the quasi-inertial solar system, on both the instantaneous equipotential of the earth's gravity field, at the level of HLS, and on the Earth's shape, along the surface where the accelerator is installed. This must be done as a function of time, in Euclidean space, with a relative precision of a few microns over 200 meters.

These effects can be modelled by taking into account Newton's Law of Universal Gravitation, and his Second Law of Motion. For a point $\mathbf{P}(x,y,z)$, the Earth's instantaneous gravity potential $\mathbf{W}_{total}(x,y,z)$ can be expressed as the sum of the gravitational potential $\mathbf{V}(x,y,z)$, the centrifugal potential $\mathbf{\Phi}(x,y,z)$ and the tidal potential $\mathbf{Tide}(x,y,z)$:

$$\mathbf{W}_{total}(x,y,z) = \mathbf{V}(x,y,z) + \mathbf{\Phi}(x,y,z) + \mathbf{Tide}(x,y,z) \quad (1)$$

As part of the CLIC feasibility study, working towards the Conceptual Design Report, two doctoral projects are analysing different aspects of this problem in order to assess what is actually possible, establish models that can be applied, determine the accuracy that can realistically be achieved, and identify the resources required.

## PRECISION GEOID DETERMINATION

Nowadays, the determination of the Earth's gravity field, especially equipotential surfaces like the geoid, is a very active and challenging domain of research for Geodesy. For example, last year, a new gravity mission (GOCE) was launched in order to increase the precision of the global geoid to 1 cm, for wavelengths down to 100 km [2]. Although these performances are amazing, the best local geoids available today are still determined by terrestrial measurements like gravity accelerations, GNSS-levelling or astro-geodetic deflections of the vertical [6]. In the best cases, wavelengths down to 1 km are known with an accuracy of a few mm to cm which is largely insufficient in the light of the CLIC alignment. Therefore, it is necessary to study the possibility and the feasibility of determining the short-wavelength

* CLIC, Compact LInear Collider.

equipotential profiles of the earth's gravity field at a level of precision of a few micrometers.

## *Theoretical Aspects*

In the following chapter, only the quasi-stationary two first terms of Eq. 1 are considered, the tidal term is treated separately. Their expansion is given in Eq. 2 and Eq. 3.

$$\mathbf{V}(x,y,z) = \iiint_{Earth} \frac{1}{r}\,\rho\left(x', y', z'\right)\cdot dV \tag{2}$$

$$\mathbf{\Phi}(x,y,z) = \frac{1}{2}\omega^2 R^2 \cdot \sin^2\varphi \tag{3}$$

where:

$r$ = distance from $\mathbf{P}(x,y,z)$ to $dV$
$\rho$ = density of $dV$
$dV$ = differential volume element
$\omega$ = Earth's rotation angular velocity
$R$ = Earth's radius
$\varphi$ = latitude of $\mathbf{P}(x,y,z)$

The quasi-static part of the Earth's gravity potential is given by [1]:

$$\mathbf{W}(x,y,z) = \mathbf{V}(x,y,z) + \mathbf{\Phi}(x,y,z) \tag{4}$$

and an equipotential is the surface where **W** is constant. The potential **W** is largely dominated by the main ellipsoidal structure of the Earth and can be separated into two distinguishable parts, which can be more easily manipulated and interpreted. **U** is a completely perfect known mathematical potential field. It is composed of a gravitational part induced by a rotational ellipsoid (large part of **V**) and the centrifugal part **Φ**. The second term **T** is called disturbing potential and represents the potential field induced by all non-modelled density anomalies in the Earth, that is the non-modelled part of **V**.

$$\mathbf{W}(x,y,z) = \mathbf{U}(x,y,z) + \mathbf{T}(x,y,z) \tag{5}$$

By definition, **U** is perfectly known; then, the precision of the determination of **W** is completely dependant of the precision of the determination of **T**. Theoretically, if the density field $\rho(x,y,z)$ (not considered by **U**) were known, **T** could be computed by applying Eq. 2. Unfortunately, only approximate density models are available and the computation of **T,** only by modelling, is directly dependent of the quality of $\rho(x,y,z)$ and is insufficient for precise applications.

Fortunately, the disturbing potential **T** can also be indirectly measured. The elements of the first and second order derivatives of **T** are accessible as observables and can be linked to equipotential surfaces or profiles. In our application, only the method of astronomical levelling can be used to reasonably reach the objective of a few microns over 200 meters [3]. Basically, by integrating Earth's surface deflections of the vertical $\varepsilon$, the geometric variations of the disturbing equipotential $\Delta N_{AB}^{H_{tnl}}$ at level $H_{tnl}$ between two points ($A$,$B$) along a profile can be expressed [3]:

$$\Delta N_{AB}^{H_{tnl}} = -\int_A^B \varepsilon \cdot ds - E_{AB}^{H_{tnl}} \tag{6}$$

with the orthometric correction:

$$E_{AB}^{H_{tnl}} = \int_A^B \frac{g-\gamma_0^{45}}{\gamma_0^{45}}\cdot dn + \frac{\bar{g}_A-\gamma_0^{45}}{\gamma_0^{45}}\cdot \Delta H_A^{tnl} - \frac{\bar{g}_A-\gamma_0^{45}}{\gamma_0^{45}}\cdot \Delta H_B^{tnl} \tag{7}$$

where:

$\varepsilon$ = deflection of the vertical on the Earth's surface projected on the profile along $A$ and $B$
$ds$ = differential length on the ellipsoid
$g$ = gravity acceleration on the Earth's surface
$\gamma_0^{45}$ = normal gravity acceleration at $\varphi = 45°$
$dn$ = differential height
$\bar{g}_{A,B}$ = mean gravity acceleration along the plumb line from $A$,$B$ to $H_{tnl}$.
$\Delta H_{A,B}^{tnl}$ = height difference between $A$, $B$ and $H_{tnl}$

In Eq. 4, it can be shown that the deflections of the vertical $\varepsilon$ are used for determination of the main part of the undulation and the gravity measurements for the computation of the orthometric correction which is equivalent to the reduction of $\varepsilon$ at level $H_{tnl}$ due to the curvature of the plumb line.

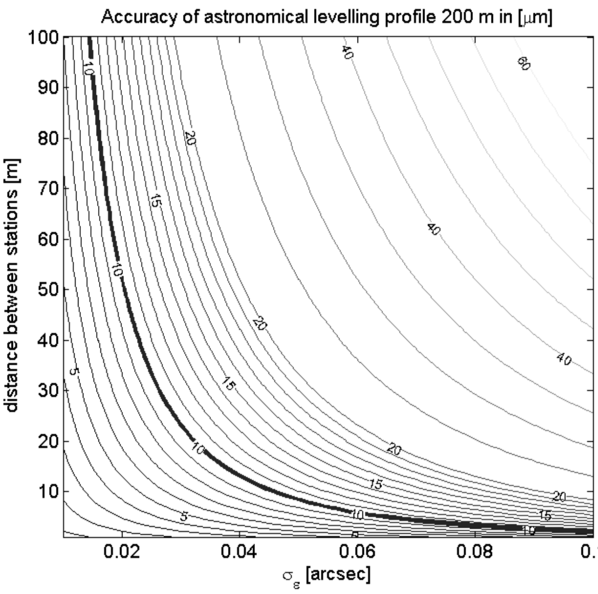


Figure 1: Simulated accuracies [μm] obtained by astronomical levelling for the variation of an equipotential profile of 200 meters length.

Usually, the computation of Eq. 6 needs the measurement of $\varepsilon$ and $g$ at discrete points along the profile from A to B. In our application thanks to the accessibility to the level $H_{tnl}$ by a tunnel, it is possible to measure $g$ directly at $H_{tnl}$ which can be used for the computation of more realistic mean $\bar{g}_{A,B}$ values along plumb lines.

In order to give an overview of achievable accuracies of astro-geodetic measurements, it is possible to estimate the precision of the determination of $\Delta N_{AB}^{H_{tnl}}$ by applying a law of variance propagation to Eq. 6. $S$ represents the distance between $A$ and $B$ and $n$ the number of deflections which are observed. Assuming that $E_{AB}^{H_{tnl}}$ is perfectly known and the deflections ε of the vertical are only affected by a gaussian white noise [3]:

$$\sigma_{\Delta N}[mm] \cong 4.8 \cdot \frac{S[km]}{\sqrt{n-1}} \cdot \sigma_{\varepsilon}['']\qquad (8)$$

## Astro-Gravimetric Measurement Campaign

In the context of feasibility studies of CLIC, an existing tunnel at CERN which has similar properties to the tunnels which are planned was chosen in order to determine an equipotential profile with the best world-wide geodetic available instrumentation. The tunnel, TZ32, is near and perpendicular to the Jura mountain chain, straight, 800 meters in length, with a diameter of 3 meters at depths between 68 and 88 meters and a slope of ~1.5 % (Fig. 2).

Deflections of the vertical and gravity measurements where carried out every 10 meters along the profile at the Earth's surface directly above the tunnel. Moreover, gravimetric measurements where also observed in the tunnel. They were carried out with the relative gravimeter Scintrex CG-5 linked to three absolute points determined by the Swiss Federal Office of Metrology METAS with the absolute gravimeter FG-5 [13].

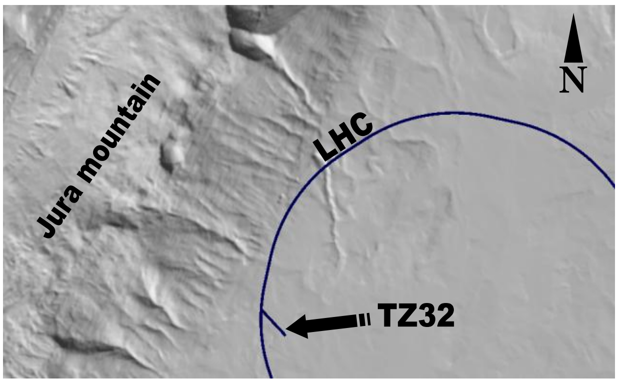

Figure 2. Perspective view of the location of the tunnel TZ32 by respect to the LHC and Jura chain.

### Astronomical Deflections of the Vertical

The deflection of the vertical measurements were carried out with the Digital Astronomical Deflection Measuring System DIADEM of ETH Zurich which is a high precision zenith camera [8]. The astronometric computations were done with the software AURIGA of the University of Hannover [4]. In order to augment the precision, the reliability, the productivity and the usability of the system in difficult field conditions, significant hardware and software improvements were made. Table 1 gives an overview of the main components of the camera.

Table 1. Principal components of DIADEM.

| Component | # type | Characteristic |
|---|---|---|
| Optic | 1x Mirotar | f=1020 mm D=200 mm |
| CCD camera | 1x Apogee Alta | 2184x1472 pixel, 6.8x6.8 microns, 16 bits |
| GPS timing | 1x ublox | precision: < 0.1 milisecond |
| Tiltmeters | 2x Wyler Zerotronics | range: +/- 3600", precision: 0.15" |
| | 4x Lippmann | range: +/- 200", precision: <0.05" |
| Digital Focuser | 1x FLI PDF | range: 0-8.9 mm, resolution: 1.3 microns |
| Automation | 3x eletric cylinders | |
| | 5x servo motors | |
| DAQ and Control | 2x computers | |

The calibration, measurement and computation processes of deflections of the vertical with a zenith camera can be found in [4], [7] and [8]. Basically, a deflection can be determined by the combination of oriented tilt measurements and the rotational direction of the telescope which is computed using the astronometric measurements of identified stars in an image of the sky. In order to eliminate principal systematic effects, one solution is the combination of measurements carried out with an azimuth difference of 180°.

In order to control and estimate the precision of the upgraded system DIADEM, a time series of deflections of the vertical were observed on a single reference point on 5 different nights. In figure 3, the time series of mean reduced south-north $\xi$ and west-east $\eta$ components are shown. The standard deviations of a single solution are 0.24 arcsec for $\xi$ and 0.26 arcsec for $\eta$, which is close to the results obtained by an equivalent system of the University of Hannover [5]. Moreover, the empirical autocorrelation function shows that single solutions are almost statistically independent. Assuming a white noise process, the precision of a deflection of the vertical based on 50 single solutions may be considered to be better than 0.1 arcsec.

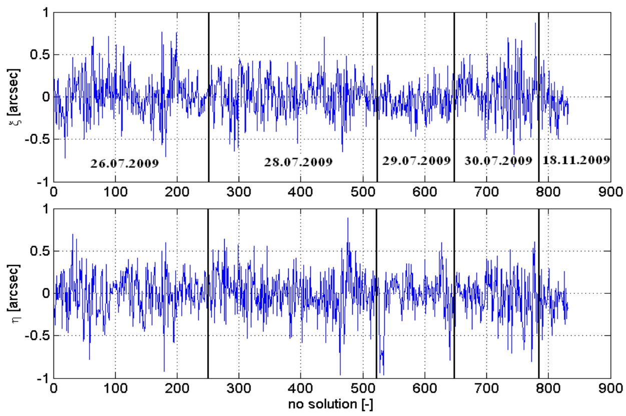

Figure 3. Time series of mean reduced ξ and η observed at CERN during 5 different nights.

*First Results of the Campaign TZ32*

As explained before, deflections of the vertical were measured every 10 meters above the TZ32 in order to determine the equipotential profile at the level of the tunnel (~425 m). The measurements were carried out during 15 nights between the 18.08.2009 and the 29.10.2009 covering the first 700 meters of the tunnel. At each station, 64 solutions were carried out in order to have a good compromise between the observation time and the precision. The deflections were computed with respect to the GRS 80 reference ellipsoid, reduced down to the first station and projected on the profile of TZ32.

For the analyses and the first comparisons of this first campaign, a simulation of the disturbed gravity field values ($\Delta N_{AB}^{H_{tnl}}$, $\varepsilon$) was performed with a software application (QGravity) developed at ETH for the computation of all gravity field components up to second order tensor based on homogenous polyhedrons for points outside and inside modeled masses [11] and [12]. For this preliminary study a simple topographic mass model was used. The disturbing density field of 2670 kg/m$^3$ was approximated by a polyhedron based on the DTM 25 of swisstopo* up to 10 km around the TZ32 and the ASTER# DEM with decreasing resolutions up to 150 km for the Earth's surface and by an piece-wise linear surface at level 0 for the bottom. The predicted deflections and the predicted variations of the equipotential are also reduced to the first point of the profile (see Fig. 4). Moreover, the predicted equipotential was tilted by an angle of +0.06 arcsec in order to mitigate the effect of the arbitrary choice of fixing the first observed deflection to 0.0 arcsec (see Fig. 5). This has no effect on the interpretation of the results.

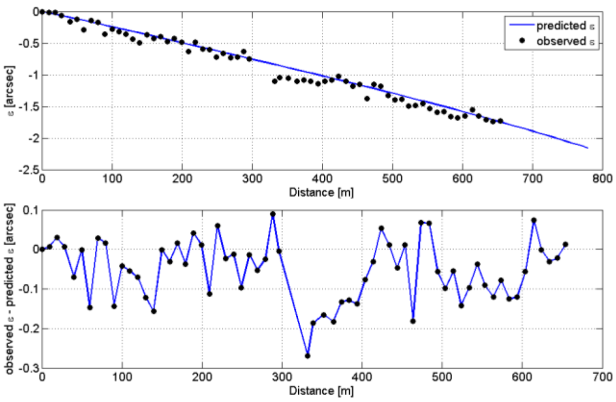


Figure 4. Predicted and measured deflections of the vertical along TZ32 (top). Differences between predicted and observed deflections (bottom).

The standard deviation of the differences between the predicted and the measured deviations of the vertical is 0.076 arcsec. This good agreement between the predicted deflections, which are only based on a mass model derived from DTM, and the purely astro-geodetic deflections of the vertical is very encouraging.

* swisstopo, Swiss Federal Office of Topography.
\# ASTER, Global Digital Elevation Model from NASA and METI.

Now, if Eq. 6 is applied, the variation of the disturbing equipotential at $H_{tnl}$ can be computed. The numerical integrations are computed with the simple algorithm of trapezoid summation and the orthometric correction term (Eq. 8) was computed using gravity measurements observed at the surface and in TZ32.

Naturally, because we don't know precisely the true shape of the equipotential and because the differences are in the order of magnitude of the achievable accuracy of the instrumentation, it is impossible to say if these differences can be interpreted as real gravity signals or not. Complementary deflections or deeper analyses of the gravimetric measurements in combination with stochastic simulations of the gravity field with improved mass models based on local geological and hydrological information should gives more indication about real signals which can be expected at this scale.

Nevertheless, this campaign shows that the expected performances of DIADEM in difficult field conditions are met and opens the possibility of the determination of high precision short-wave length equipotentials.

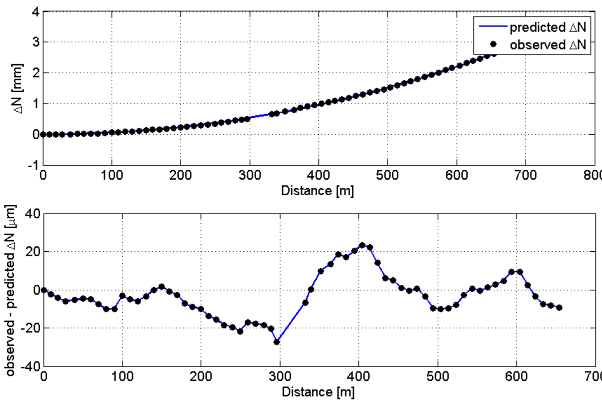


Figure 5. Predicted and measured variation of the disturbing equipotential at $H_{tnl}$ (top). Differences between predicted and observed $\Delta N_{AB}^{H_{tnl}}$ (bottom).

However, better analyses of potential systematical effects such as anomalous refraction [6] which can affect the astro-geodetic measurements and the construction of smaller, more transportable and faster zenith camera systems are necessary in the perspective of the measurement of a profile of 50 km.

## TIDAL EFFECTS ON HLS NETWORKS

The HLS used for accelerator alignment are sufficiently accurate and stable to be affected by tidal and other effects. This can be seen from Fig. 6 which shows readings from 3 HLS sensors along a 140 m test network installation changing with a period of 12 and 24 hours. These periodic variations in the measurements are primarily explained by Earth tides. The relative motions of the different bodies in our solar system (principally the Sun the Moon) with respect to the Earth, deforms both the Earth's crust and the HLS water surface through the potential tide [14], Eq. 1.

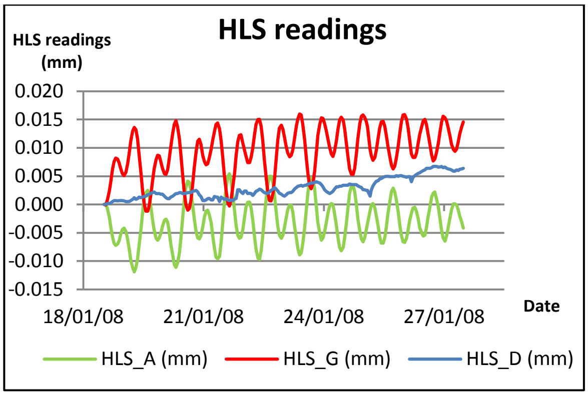


Figure 6: Raw Readings of 3 HLS sensors

The effect of the potential tide on different instruments is modelled by the determination of specific Love Numbers. As mentioned above, the crust Tilt tide, which is measured by an HLS, has two components, and in the literature, (16), (17), is represented by the following Love Number combination:

$$\gamma = 1 + k - h \qquad (9)$$

The expected tidal affect defined by these numbers is disturbed at various scales by phenomena such as the topography, and anomalies in the mass density of the earth. With a sufficiently large number of continuous measurements it is possible to determine the small corrections that need to be applied to these Love Numbers for a given HLS installation.

In the context of the alignment of any accelerator, and more specifically the CLIC project [19] with the requirement to align all the components in a 200 m window with a relative accuracy of several microns, it is important to be able to distinguish and model those elements of the tides which would have no effect on the relative alignment because they cause a homogeneous tilt, and those which will cause a local deformation.

The goal for the processing of the HLS measurements is therefore to isolate the local ground deformations from the raw measurement signal. The components of the raw measurement signal are given in Eq. 10.

Ground Deformation = Raw HLS Signal – Tide Effects
- Load Effects
- Residual Perturbations *(10)*

The best known and most extensive tool for the analysis and prediction of tidal effects is an application called Eterna, [15]. This software was developed by Hans-Georg Wenzel in the 90s. It has several modules, one of which is able to predict the theoretical tilt crust tide (combination of crust tide and potential tide) at any point and in any azimuth (Predict Module). Another module is able to compare theoretical model of tides against a set measurements and give wave by wave amplitude factor and phase shift parameters to best characterize the local tide signal (Analyze Module). This program has been the main tool used throughout this project.

## *Tidal and other Influences*

An effort has been made to identify all the Tidal and other influences on a given set of HLS measurements. These phenomena have been grouped and presented in Table 2. The idea behind this table is to identify how the different effects contribute to the HLS measurement signal.

If we consider Eq. 10 again, the Ground deformation has four potential sources:

- Cavity effects here represent the deformation of the accelerator tunnel under the influence of the Earth Tides. It is a function of the size and structure of the tunnel as well as the surrounding rock (concrete thickness, presence of a nearby gallery);
- Topography effects represent the modifying effect of the ground structure on the tides (an amplification or attenuation depending on the location);
- Permanent deformation refers to a local shift in the ground structure, typically caused by a fault, or changes in underground water levels;
- Periodic temperature changes refer to the effect on the tunnel of daily temperature variations driven by the sun, heating or ventilation (temperature difference between day and night).

Table 2: Tidal and other influences that affect HLS measurements

| | Tilt | | Deformation | |
|---|---|---|---|---|
| | Ground | Instrument | Ground | Instrument |
| Periodic | Crust Tide Periods of 12 & 24h | Equipotential Tide Periods of 12 & 24h | Cavity effects Periods of 12 & 24h | Temperature Periods of 24h |
| | | | Temperature Periods of 24h | |
| | Oceanic load Periods of 12 & 24h | Specific response of the water network Periods of 12 & 24h | Topography effects Periods of 12 & 24h | |
| No periodic | Atmospheric load | | Permanent deformation | Temperature |
| | Hydrological load | | | |
| Static | | | | Geoid |

The Tide Effect has two components, which can be modeled independently or together with the Eterna software. The two tides are:

- The Crust Tide – the tide effect on the height;
- The Equipotential Tide – the potential tide applied to the surface on the water in the HLS.

The load effects are repercussions of physical phenomena which result in significant short term changes in the mass distribution of the Earth. They deform the Earth's crust and can be coupled with tides. The load effects are listed below:

- Oceanic load represents the result of the tidal movement of the oceans;
- Atmospheric load is the result of changes in the atmospheric pressure;
- Hydrological load is the result of changes in water levels of lakes, underground water tables or soil moisture content.

The residual perturbations represents a catch all category for those effects not already classified. They include:

- The specific response of the water network as the water in the HLS responds to the tides and other forces (moving wave, amortization of the network);
- Periodic temperature changes which have an effect on the HLS instrument such as daily temperature variations driven by the sun, heating or ventilation (temperature difference between day and night);
- Non-periodic temperature changes caused by events in the area around our instrumentation (e.g. opening a door);
- The geoid - an instantaneous view of an equipotential surface of the Earth's gravity field which can be used to determine the corresponding form of the water surface in the HLS.

In order to determine the Ground Deformation, it is clear from Eq. 10 that we must determine all the elements on the right hand side of the equation. For the moment it is considered that over a 200 m distance the geoid is smooth and it is not considered in the following analyses. The first part of this paper describes the work being carried out to define a high precision geoid, and the models resulting from this work can be integrated if necessary once they have been determined. We obviously have the raw measurements, and different approaches are possible for determining the remaining elements.

## *Network Analysis*

A typical approach to correct HLS signal from tides and other periodic effects is to use the Analyze module of the Eterna application. This module compares the raw measurement signal against the theoretical model of the tides. It modifies the tide parameters, and gives phase shift and amplitude parameters values to predict future local tides in the same area with the same instrument. The disadvantage is that in calculating this model, Eterna cannot distinguish the other periodic effects identified in Table 2, and listed below:

- Oceanic load;
- Specific response of the water network;
- Cavity effects;
- Topography effects;
- Diurnal temperature on ground and instrument.

Our initial decision was nonetheless to follow this approach, and the Eterna Analyze Module was used to process a 2.5 month set of HLS measurement data from our test network. The results from this analysis were then fed back into the Eterna Predict Module, and produced a predicted tidal signal, specific to the test network, covering a later 3 week period. This predicted tidal signal was then used in the subsequent analysis together with results for the load effects, which were kindly calculated and provided Jean Paul Boy*.

The adopted procedure was to take the raw HLS signal and remove the predicted signals. If the predicted signals are removed one by one we can perform some analysis to quantify the improvement between the start signal and the end signal at each step. The details of the procedure are as follows:

- Calculate the standard deviation of the start and predicted signals;
- Calculate the correlation between the predicted signal and the start signal;
- Remove the predicted signal from the start signal;
- Calculate the standard deviation of the end signal.

At the end of the procedure the end signal becomes the new start signal and the next predicted signal is processed. The tide effects and load effects are both processed in this way. The analyses of the results from the processing of 3 weeks of height difference measurements signal (dH) from an HLS (the 2 sensors are separated from 140m) are given in Table 3.

Table 3: Results from the Network Analysis

| Signal | Stdev of this signal (mm) | Correlation betwen this signal and the previous raw (%) | Stdev of the signal after correction (mm) |
|---|---|---|---|
| Raw HLS Signal [1] | 0.0071 | X | X |
| Predicted tide [2] | 0.0056 | 80 | 0.0043 |
| Atmospheric load [4] | 0.0009 | 52 | 0.0039 |
| Hydrological load [4] | 0.0002 | 45 | 0.0039 |

The order in which the predicted tides are listed in Table 3 is indicative of the order in which they were removed from the raw HLS signal. The idea was to remove the largest signal first, since this would give the best estimate for the correlations between the start signal and the predicted signal. None of the periodic signals have been explicitly removed from the raw HLS signal,

* J.P. Boy, Greenbelt, USA : s.n., 2010. NASA GSFC.

since they should be modelled by Eterna.

After this procedure has been applied to the raw HLS signal the residual signal (the final end signal) can be seen in Fig. 7 and an FFT analysis of the measurement signal and the residual signal is given in Fig. 8. The main periods that are shown by the FFT analysis are 12.3 h and 24.0 h. After the predicted signals have been removed, the amplitudes of these two periodic effects have been reduced by a factor of 6 and 5 respectively.

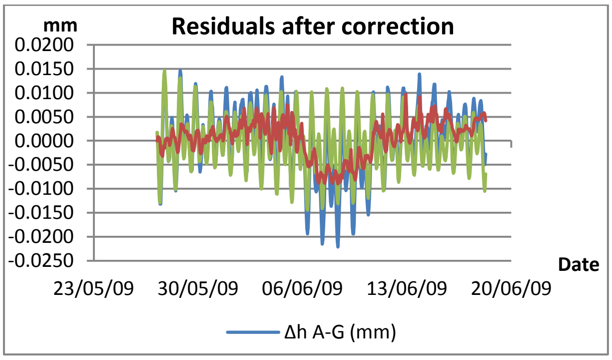


Figure 7: Residual Signal after Network Analysis

This residual signal can be considered to be the ground deformation, but it is worth noting a number of points. Firstly as has already been mentioned some of the ground deformation should have been removed by the Eterna predicted tide signal. Secondly from Fig. 7 we can see that in the central part of the period being analysed the residual curve follows the trend of the initial signal, indicating that the model here does not fit very well with the raw HLS signal.

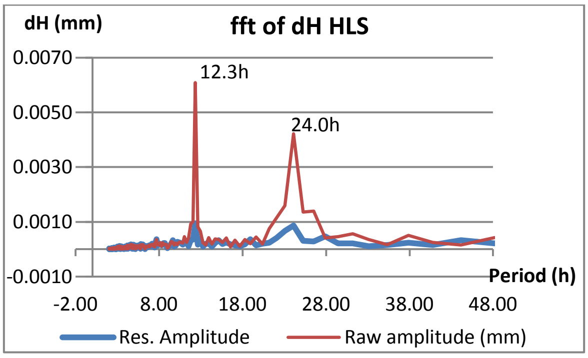


Figure 8: FFT for Network Analysis

There are improvements which can be made to this analysis procedure which we would expect to improve these results. The first step would be to remove as many signal or corrections as possible from the measurements which are run through the Analyse Module. This applies in particular to the load effects and the Temperature effects since these are not likely to be the same in subsequent periods. This also means that the Oceanic Load and the Temperature effects should be removed from the raw HLS signal used at the prediction stage.

The major disadvantage of this approach however, is the fact that part of the ground deformation signal, which we are trying to determine, has been removed by the analysis process. This led us to try an alterative approach.

## *Analytical Prediction*

The analytical prediction approach to solving Eq. 10 involves using existing models for the tides and the perturbing signals. The theoretical models in the Predict module of Eterna have been used for predicting the tides, thermal expansion coefficients and structural designs have been used to model changes in the HLS instrument with changes in temperature, and again the results for the loas effects are those kindly provided by Jean Paul Boy.

With these predicted signals the procedure for processing the raw HLS signal is exactly the same as that emplyed for the Network Analysis above.

The analyses of the results from the processing of the same 3 weeks of HLS height difference measurements signal (dH) are given in Table 4.

Table 4: Results from the Analytical Prediction

| Signal | Stdev of this signal (mm) | Correlation between this signal and the previous raw (%) | Stdev of the signal after correction (mm) |
|---|---|---|---|
| Raw HLS Signal [1] | 0.0071 | X | X |
| Predicted tide [2] | 0.0047 | 79 | 0.0045 |
| Temperature effect [3] | 0.0040 | 68 | 0.0034 |
| Tidal Oceanic load [4] | 0.0008 | 36 | 0.0032 |
| Atmospheric load [4] | 0.0009 | 43 | 0.0030 |
| Hydrological load [4] | 0.0002 | 56 | 0.0029 |

It is clear from Table 4 that the specific response from this HLS water network has not been taken into account. A partnership has been developed with the Université de Montpellier in France, and, following a number of tests to characterise this network, we hope to have a model of the instrumental response in October.

After this procedure has been applied to the raw measurement signal the residual signal can be seen in Fig. 9 and an FFT analysis of the measurement signal and the residual signal is given in Fig. 10.

The raw measurement signal presents maximum periodic amplitudes of +/-15 µm; the residual signal presents maximum periodic amplitudes of +/-4 µm. The main periods that are shown by the FFT analysis are 12.3 h and 24.0 h. After the predicted signals have been removed, the amplitudes of these two periodic effects have been reduced by a factor of 8 and 3 respectively.

There remains a small periodic residual, mainly on diurnal wave, which could be explained by the diurnal temperature effect on the instrument (which could be calculated and applied) and on the ground via the building. This latter effect is part of the ground deformation listed above, and has therefore not been removed since because we want to keep this signal, to realign an accelerator for example.

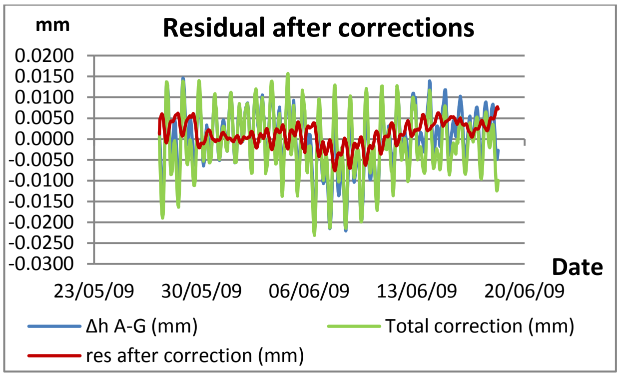


Figure 9: Residual Signal after Analytical Prediction

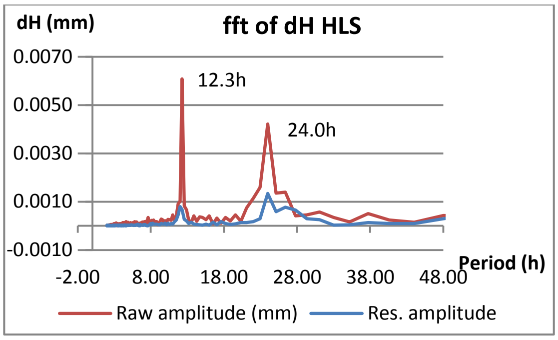


Figure 10: FFT for Analytical Prediction

Regarding the magnitude of the periodic signal which remains in the ground deformation signal, the two methods are similar. However in this Analytical Prediction method the dispersion of the signal is smaller. We can also see that in the central part of the period being analysed the predicted signal fits the raw HLS signal much better, probably because additional predicted signals are included.

This method still presents a disadvantage which must be addressed. We now have a ground deformation signal which we could apply, but we cannot identify whether this signal represents local deformations or just a global tilt applied to the area of the test installation.

### *A New Alternative Approach*

A proposition has been made for a new alternative approach to address the problem particular to the use of these systems for accelerator alignment, namely to identify the signal for any local deformations. This method also takes into account the fact that HLS networks for accelerator alignment necessarily include more than two sensors in each network. This method involves processing at least 3 aligned HLS sensors. Using the Analyze Module we make an analysis of the pair of sensors at each end of the network. This allows us to calculate a long base which we shall assume defines the global movements (tilts) of the area being studied. Using one end point sensor and each of the intermediate sensors in turn we perform an analysis of each pair of sensors in turn. For each pair of sensors the modelled signal should now represent the global movements plus the local effects. In theory, the subtraction of the two models eliminates the global movements (constant on a same area) to give just the local effects at the intermediate sensor. This analysis is now underway.

## CONCLUSION

To address questions raised by the CLIC feasibility study, and also to improve the pre-processing of HLS measurements from the installations in the LHC, two doctoral study programs have been launched. Both research projects are now in their final year and we are beginning to get the first results and identify the areas where further work is needed.

Campaigns of astro-geodetic measurements and gravimetric measurements have been carried out in order to determine the deflection of the vertical values along an 800 m tunnel connected to the LHC ring. Initial results are very promising, but further work is required to statistically confirm the results obtained.

Two different approaches to determining the ground deformations from HLS measurements have been tried. As we have better understood the information we are looking to extract from the HLS signal it has become clear that both methods have drawbacks that should be addressed. A third alternative approach is now proposed which should address those drawbacks. The application of this alternative methodology is in the process of being tested.

It would seem that we are close to being able to identify how to determine a high precision geoid model in an accelerator tunnel, and also how to model the temporal changes in that geoid in order to fully exploits our HLS. It will then be necessary to take a pragmatic look at both solutions and decide how this can be applied to the LHC HLS installations and the CLIC project.

## REFERENCES

[1] W. Torge, “Geodesy”, 3rd Edition, de Gruyter, (2001);
[2] ESA, “Gravity Field and Steady-State Ocean Circulation M ission”, ESA, SP-1233, (1999);
[3] C. Hirt, “Hochauflösende astrogeodätische Bestimmung von Geoid- und Aequipotentialprofilen mit Submillimetergenauigkeit für die Vermessung von Teilchenbeschleunigern”, AVN, (2008);
[4] C. Hirt, “ Entwicklung und Erprobung eines digitalen Zenitkamerasystems für die hochpräzise Lotabweichungsbestimmung“, Wissenschaftliche Arbeiten der Fachrichtung Geodäsie und Geoinformatik an der Universität Hannover Nr. 253, (2004):
[5] C. Hirt, G. Seeber, ”Accuracy Analysis of vertical deflection data observed with the Hannover Digital

Zenith Camera System TZK2-D”, Journal of Geodesy 82, (2008);
[6] C. Hirt, “Monitoring and analysis of anomalous refraction using a digital zenith camera system“, Astronomy & Astrophysics 459, (2006);
[7] C. Hirt, B. Bürki, “Status of Geodetic Astronomy at the Beginning of the 21st Century”, Univ.-Prof. Dr.-Ing. Prof. h.c. Günter Seeber anlässlich seines 65. Geburtstages und der Verabschiedung in den Ruhestand, (2006);
[8] A. Somieski, “Astrogeodetic Geoid and Isostatic Considerations in the North Aegean Sea, Greece“, Diss. ETH No. 17790, (2008);
[9] B. Wirth, “Höhensystem, Schwerepotential und Niveauflächen”, Geodätische-geophysikalische Arbeiten in der Schweiz, (1990);
[10] U. Marti, “Geoid der Schweiz“, Geodätische-geophysikalische Arbeiten in der Schweiz, (1997);
[11] D. Tsoulis, S. Petrovic, “On the singularities of the gravity field of a homogeneous polyhedral body “, Geophysics 66, (2001);
[12] S. Petrovic, “Determination of the potential of homogeneous polyhedral bodies using line integrals”, Journal of Geodesy 77, (1996);
[13] H. Baumann, “Rapport de mesure No 131-01085,…, 131-01085”, METAS, (2009) ;
[14] L. Longuevergne, “Contribution à l’hydrogéodésie”, UPMC. Paris, France, 2008. p. 16, PhD thesis.
[15] W. Torge, “The 2nd ETC Medal Award”; http://www.geo.uni-jena.de [Online] march 2000; http://www.geo.uni-jena.de/geophysik/etc/wenzel.html.
[16] H. Legros, “Sur quelques problèmes de dynamique planétaire”, ULP. Strasbourg, France , 1987. PhD thesis.
[17] P. Melchior, “THE EARTH TIDES [ed.] ”, Permagon Press. Brussels , 1966.
[18] T. Touzé, “Feasibility of the CLIC metrological reference network”, Genève, Switzerland , 2010. IWAA 2010.